AGU PUBLICATIONS

JGR

Journal of Geophysical Research: Atmospheres

RESEARCH ARTICLE
10.1002/2016JD024900

Key Points:
- The median current peaks associated with RS-type ICC pulses and return strokes are, respectively, 3.4 kA and 8 kA
- The associated median radiation E-field peaks normalized to 100 km are 1.5 V/m and 4.4 V/m, for ICC pulses and return strokes, respectively
- Comparison of RS-type ICC pulses and return strokes suggests that the former are associated with the mixed mode of charge transfer to ground

Correspondence to:
F. Rachidi,
farhad.rachidi@epfl.ch

Citation:
Azadifar, M., F. Rachidi, M. Rubinstein, V. A. Rakov, M. Paolone, D. Pavanello, and S. Metz (2016), Fast initial continuous current pulses versus return stroke pulses in tower-initiated lightning, *J. Geophys. Res. Atmos.*, *121*, 6425–6434, doi:10.1002/2016JD024900.

Received 4 FEB 2016
Accepted 20 MAY 2016
Accepted article online 23 MAY 2016
Published online 9 JUN 2016

Fast initial continuous current pulses versus return stroke pulses in tower-initiated lightning

Mohammad Azadifar[1], Farhad Rachidi[1], Marcos Rubinstein[2], Vladimir A. Rakov[3], Mario Paolone[4], Davide Pavanello[5], and Stefan Metz[6]

[1]Electromagnetic Compatibility Laboratory, Swiss Federal Institute of Technology (EPFL), Lausanne, Switzerland, [2]University of Applied Sciences of Western Switzerland, Yverdon-les-Bains, Switzerland, [3]Department of Electrical and Computer Engineering, University of Florida, Gainesville, Florida, USA, [4]Distributed Energy Systems Laboratory, Swiss Federal Institute of Technology (EPFL), Lausanne, Switzerland, [5]University of Applied Sciences of Western Switzerland (HES-SO), Sion, Switzerland, [6]Huber+Suhner AG, Herisau, Switzerland

Abstract We present a study focused on pulses superimposed on the initial continuous current of upward negative discharges. The study is based on experimental data consisting of correlated lightning current waveforms recorded at the instrumented Säntis Tower in Switzerland and electric fields recorded at a distance of 14.7 km from the tower. Two different types of pulses superimposed on the initial continuous current were identified: (1) *M*-component-type pulses, for which the microsecond-scale electric field pulse occurs significantly earlier than the onset of the current pulse, and (2) fast pulses, for which the onset of the field matches that of the current pulse. We analyze the currents and fields associated with these fast pulses (return-stroke type (RS-type) initial continuous current (ICC) pulses) and compare their characteristics with those of return strokes. A total of nine flashes containing 44 RS-type ICC pulses and 24 return strokes were analyzed. The median current peaks associated with RS-type ICC pulses and return strokes are, respectively, 3.4 kA and 8 kA. The associated median E-field peaks normalized to 100 km are 1.5 V/m and 4.4 V/m, respectively. On the other hand, the electric field peaks versus current peaks for the two data sets (RS-type ICC pulses and return strokes) are characterized by very similar linear regression slopes, namely, 3.67 V/(m kA) for the ICC pulses and 3.77 V/(m kA) for the return strokes. Assuming the field-current relation based on the transmission line model, we estimated the apparent speed of both the RS-type ICC pulses and return strokes to be about 1.4×10^8 m/s. A strong linear correlation is observed between the E-field risetime and the current risetime for the ICC pulses, similar to the relation observed between the E-field risetime and current risetime for return strokes. The similarity of the RS-type ICC pulses with return strokes suggests that these pulses are associated with the mixed mode of charge transfer to ground.

1. Introduction

Upward lightning discharges initiated from tall structures have been studied using instrumented towers in different countries. Lightning current waveforms associated with a negative upward discharge begin with the initial stage including a slowly varying current waveform called initial continuous current (ICC), which might be accompanied by superimposed pulses called ICC pulses. After the extinction of the ICC and a no-current interval, the initial stage can be followed by one or more downward-leader-return-stroke sequences, similar to those in downward lightning discharges can occur [*Rakov and Uman*, 2003]. A comprehensive study on the initial stage of negative upward flashes has been reported in *Miki et al.* [2005].

Analyses of parameters of negative upward lightning flashes using data from instrumented towers have been presented for instance, in *Diendorfer et al.* [2009], *Heidler et al.* [2013], *and Romero et al.* [2013]. Tower data along with simultaneous observations of electromagnetic fields at close distances of 170 m to 189 m [e.g., *Heidler et al.*, 2013; *Fuchs et al.*, 1998; *Diendorfer*, 2010; *Zhou et al.*, 2015] have been obtained. Video observations have also been used to investigate the initiation mechanism and various processes of upward flashes [e.g., *Miki et al.*, 2012; *Flache et al.*, 2008; *Mazur and Ruhnke*, 2011; *Qie et al.*, 2011; *Winn et al.*, 2012].

Miki et al. [2005] examined the characteristics of the ICC pulses in tower-initiated and rocket-triggered lightning and found that ICC pulses in tower-initiated lightning exhibit larger peaks, shorter risetimes, and shorter half-peak widths than do ICC pulses in triggered lightning. Two reasons were proposed to explain the observed differences: (1) the presence of multiple upward branches facilitating the occurrence of a continuous

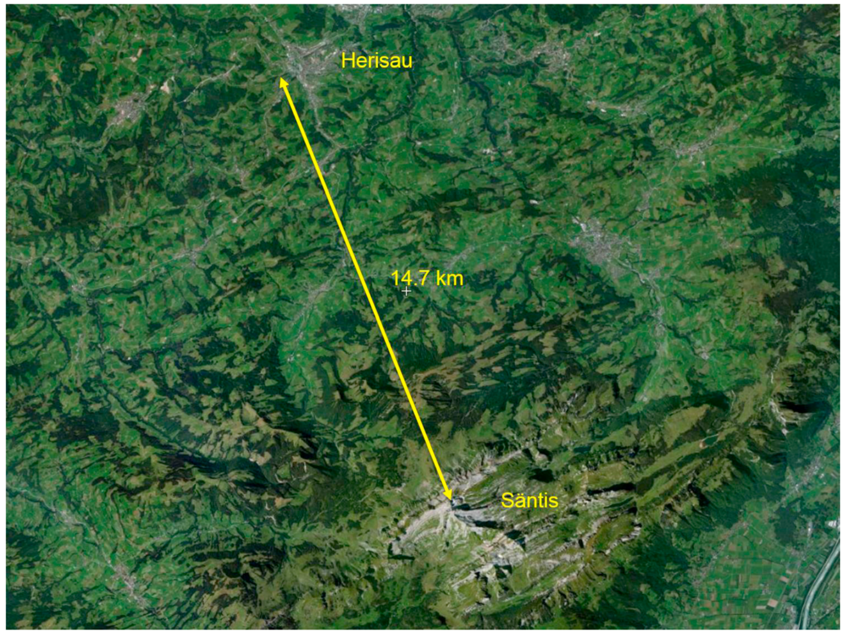

Figure 1. Locations of the Säntis Tower and the field measurement station in Herisau (Northeastern Switzerland).

current in one branch and a downward leader in another branch and (2) the fact that the charge sources in thunderclouds or branching points for ICC pulses might be located closer to the tall structures than their counterparts in triggered lightning experiments [*Zhou et al*., 2015]. *Flache et al*. [2008] analyzed high-speed video images and current records of upward discharges initiated by the Peissenberg Tower in Germany. Their study supports the hypothesis according to which ICC pulses with relatively long risetimes (greater than 8 μs) are associated with the *M*-component mode of charge transfer, while those with relatively short risetimes (shorter than 8 μs) are associated with the return stroke mode of charge transfer. A similar analysis but additionally involving close electric field measurements was made more recently by *Zhou et al*. [2015] on data from the Gaisberg Tower. *Zhou et al*. [2015] used the term mixed mode of charge transfer to ground for ICC pulses associated with the occurrence of leader/return stroke mode charge transfer in a decayed or newly formed channel connected at low altitude to the ICC-carrying channel (see Figure 15 of *Zhou et al*. [2015]).

Unlike previous data associated with instrumented towers, in which fields only at relatively close distances up to 190 m are generally available, we present simultaneous measurements of lightning currents and relatively distant fields at about 15 km, associated with pulses superimposed on the channel base initial continuous current in upward flashes. It is worth noting that simultaneous records of currents and distant (45 km) electric fields associated with *M*-component processes in rocket-triggered lightning have been reported by *Tran et al*. [2013]. Also, *Pichler et al*. [2010] presented a set of simultaneous records of current and far (79 km) fields associated with an *M*-component-type ICC pulse of an upward flash from the Gaisberg Tower.

Two different types of pulses superimposed on the initial continuous current can be identified: (1) *M*-component-type pulses which are very similar to the pulses presented in *Rakov et al*. [2001] and (2) fast pulses which are very similar to return stroke pulses. These fast pulses have been commonly observed in current records of upward flashes from tall structures, but relatively rarely in rocket-triggered lightning (see Figure 9b of *Mallick et al*. [2014]).

In this study, we present an analysis of electric fields radiated by fast ICC pulses, in comparison with those associated with return strokes. Use is made of simultaneous records of lightning currents and electric fields associated with upward negative flashes initiated from the Säntis Tower. The field sensors were located at a distance of about 14.7 km from the tower. At this distance, the initial electric field peak for return strokes is essentially due to the radiation field component.

The paper is organized as follows. Section 2 briefly presents the instrumentation. Section 3 presents an overview of the obtained data, followed by a comparison between some characteristics of radiated fields

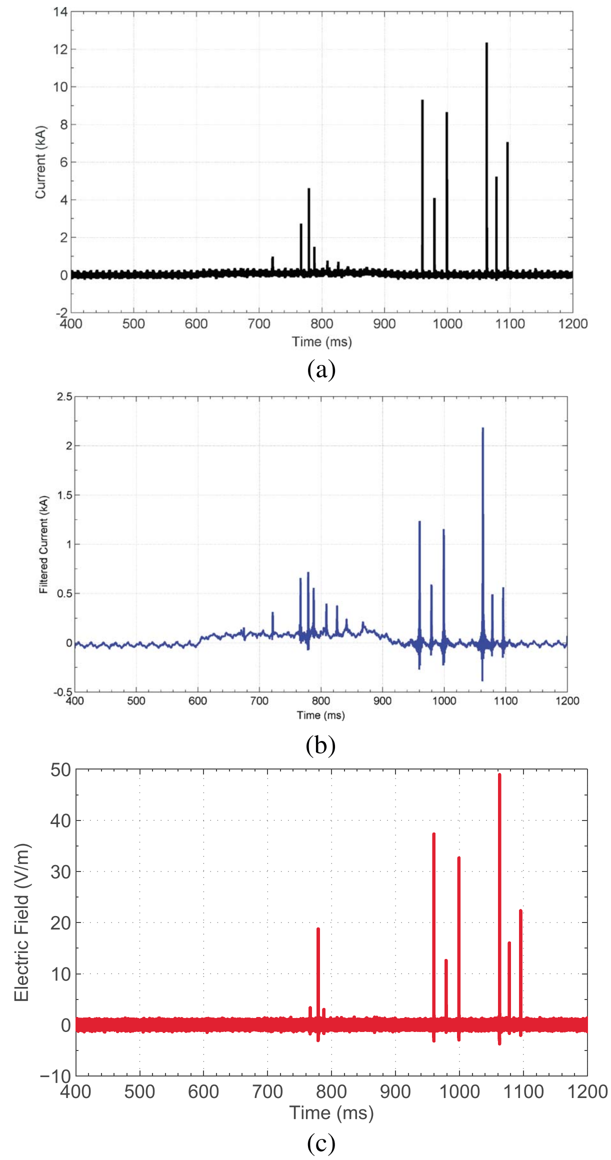

Figure 2. Waveforms associated with a flash occurred on 22 October 2014 at 1:14 A.M. (a) Original current waveform. (b) Current waveform filtered with 1 kHz low-pass filter. (c) E-field waveform at 14.7 km.

associated with ICC pulses and return strokes. A discussion on the obtained results is presented in section 4. Summary and conclusions are given in section 5.

2. Instrumentation

The current measurement system of the Säntis Tower (located in the northeast of Switzerland) has been operational since May 2010. Lightning current waveforms and their time derivatives are measured at two different heights (24 m and 82 m above ground level) using Rogowski coils and multigap B-Dot sensors. More details on the deployed measurement system of the Säntis Tower can be found in *Romero et al.* [2012] and *Azadifar et al.* [2014].

A temporary station for measuring wideband electric fields associated with flashes striking the Säntis Tower was deployed on 23 July 2014 and was operational until 28 October 2014. The system included two Thales (former Thomson CSF) Mélopée sets for the measurement of vertical electric fields and azimuthal magnetic fields. Each set included a sensor, a conditioner, fiber optic connection, and a receiver. The operating frequency bandwidth of the system was 2 kHz to 150 MHz. A PCI platform with sampling rate of 50 MS/s was used to digitize and record the field waveforms. The electric and magnetic field sensors were installed on the roof of a 25 m tall building (Huber+Suhner) in Herisau, 14.7 km away from the Säntis Tower. It should be noted that the GPS timestamping was not present at the time of the field measurement campaign, and field and current data are aligned using the last return stroke of each flash, which can provide precise alignment with an error in the order of few microseconds.

Figure 1 shows the locations of the Säntis Tower and the field measuring station.

3. Data

3.1. Overall Waveform Characteristics

During the operation of the field measurement station (23 July to 28 October 2014), a total of 26 flashes were simultaneously recorded at the Säntis Tower and at the Herisau field station. Out of these 26 flashes, 21 were negative. An analysis of the recorded positive flashes is presented in *Azadifar et al.* [2015].

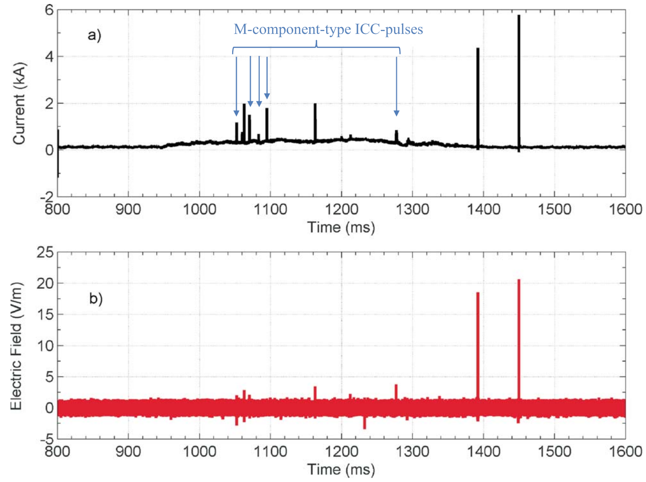

Figure 3. Waveforms associated with a flash that occurred on 22 October 2014 at 00:56 A.M. (a) Current waveform. (b) E-field waveform at 14.7 km.

Figure 2a presents the current waveform associated with an upward negative flash that occurred on 22 October 2014 at 1:14 A.M.. Figure 2b shows the filtered waveform using a low-pass zero-phase filter with a cutoff frequency of 1 kHz. In the filtered waveform, one can clearly distinguish the ICC (with six superimposed pulses), followed by six return strokes. Figure 2c presents the associated electric field waveform. Note that the electric field waveforms have been shifted in time to align the return stroke pulses with their current counterparts.

It should be noted that the atmospheric electricity sign convention is used in this study for the electric field data and that a positive sign is used for the current waveform associated with negative return strokes, which effectively transfer positive charge upward or, equivalently, negative charge to the ground.

3.2. Observed ICC Pulses

As mentioned in the Introduction, two different types of ICC pulses were observed in our measurement results.

M-component type pulses. These pulses are characterized by a slow waveform with risetimes of the order of a few hundreds of microseconds. Figure 3 shows the current waveform associated with an upward negative flash that occurred on 22 October 2014 at 00:56 A.M., in which *M*-component-type ICC pulses are marked with blue arrows. Figure 4 presents an expanded view of the current and field waveforms of one ICC pulse of this type, which occurred at a time of about 1276 ms. It can be seen that the microsecond-scale electric field pulse occurs about 120 μs prior to the onset of the current pulse. This time shift is in agreement with observations in *Rakov et al*. [2001], *Tran et al*. [2013], and [*Pichler et al*., 2010], in which the microseconds-scale field pulse was attributed to intracloud activity preceding and possibly initiating the *M* component.

Return-stroke type pulses. Figure 5 shows an expanded view of the current and field waveforms of an ICC pulse of this type in the flash shown in Figure 2. The current is characterized by a peak value of 4.6 kA and a 10–90% risetime of 2.1 μs. The corresponding E-field peak is 21.4 V/m, and the E-field risetime is 2.3 μs. As can be seen, unlike the *M*-component type pulse shown in Figure 4, the onset of the field matches that of the current pulse, indicating that the source of radiation is near the base of the channel. Furthermore, the radiated electric field pulse appears to be similar to radiated fields associated with return strokes. This can be seen by examining Figure 6, which shows an expanded view of the current and field waveforms of a return stroke in the same flash. The current has a peak value of 9.4 kA and a 10–90% risetime of 1.0 μs, and the E-field has a peak value of 40.7 V/m and a risetime of 2.0 μs. In the next section, we will present a more detailed comparison between return-stroke type (RS-type) ICC pulses and return strokes.

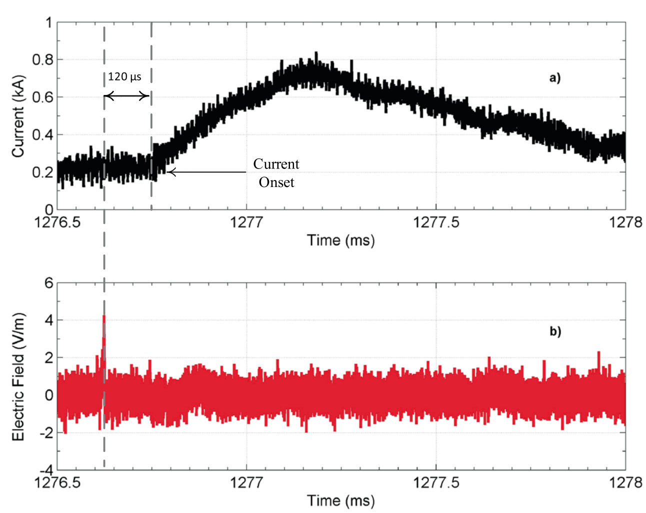

Figure 4. Expanded view of the *M*-component-type ICC pulse that occurred in the flash shown in Figure 3. (a) Current pulse. (b) E-field pulse at 14.7 km.

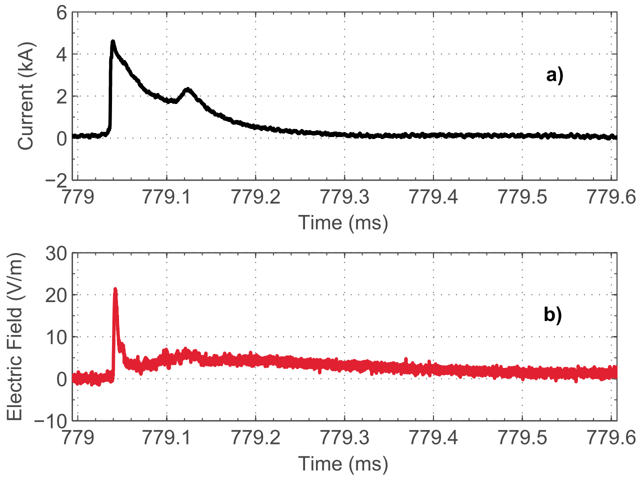

Figure 5. Current and E-field waveforms associated with an RS-type ICC pulse in the flash that occurred on 22 October 2014 at 1:14 A.M. (Figure 2). (a) Current. (b) E-field.

4. Comparison of RS-Type ICC Pulses and Return Stokes

In the present study, current and E-field waveforms from nine upward flashes (out of the 21 recorded) were examined. Twelve flashes were discarded from the analysis because their current waveform contained at least one pulse that could not be classified unequivocally as ICC pulse or return stroke. Typically, these pulses occurred either at the very end of the ICC or very shortly after its extinction. Using the same low-pass filtering technique applied to the flash shown in Figure 2, the ICC ending times were evaluated for the nine flashes, and based on this evaluation, the recorded pulses were classified either as RS-type ICC pulses or as return strokes. It should be mentioned that in the analysis, pulses with peak amplitudes lower than 1 kA for the current or 2 V/m for the field were ignored in this study due to uncertainties associated with the extraction of the parameters of these low-peak pulses. Applying the aforementioned criteria, a total number of 44 RS-type ICC pulses and 24 return strokes were identified.

In this section, individual characteristics of RS-type ICC pulses and return strokes are investigated. Figure 7 shows the scatterplot of peak E-field versus peak current for all considered RS-type ICC pulses (blue circles) and return strokes (red circles).

It can be seen that the RS-type ICC pulses have, in general, smaller current and field peaks compared to return strokes. On the other hand, the two data sets are characterized by very similar linear regression slopes, namely, 3.67 V/(m· kA) for the ICC pulses and 3.77 V/(m kA) for return strokes. It should be noted that regression lines are forced to go through the origin. Assuming the field-current relation based on the single-wave transmission line (TL) model (e.g., [*Rachidi and Thottappillil*, 1993]), and considering a factor of 2 (discussed below) accounting for the enhancement of the electric field associated with the mountainous profile of the field propagation path, the estimated value for the apparent speed of both RS-type ICC pulses and return strokes is about 1.4×10^8 m/s, which is in agreement with the reported range of values (about one third to half the speed of of light) found for return strokes in other studies [*Rakov* 2007]. Strictly speaking, the single-wave TL model is not applicable to ICC pulses that, in general, involve two overlapping waves, but we believe that for fast ICC pulses the upward (RS-like) wave is dominant, as further discussed in section 5.

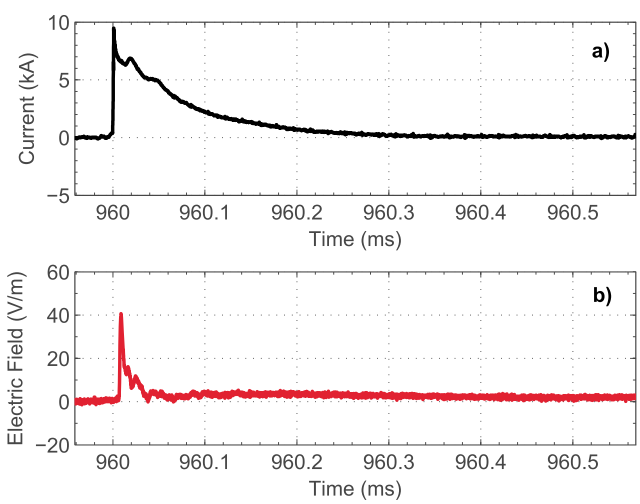

Figure 6. Current and E-field waveforms associated with a return stroke in the flash that occurred on 22 October 2014 at 1:14 A.M. (Figure 2). (a) Current. (b) E-field.

A discussion is in order on the adopted factor 2 in the estimation of the apparent speed of RS-type ICC pulses and return strokes. *Li et al.* [2016] presented an finite difference time domain analysis of the field propagation using simultaneous records of lightning currents

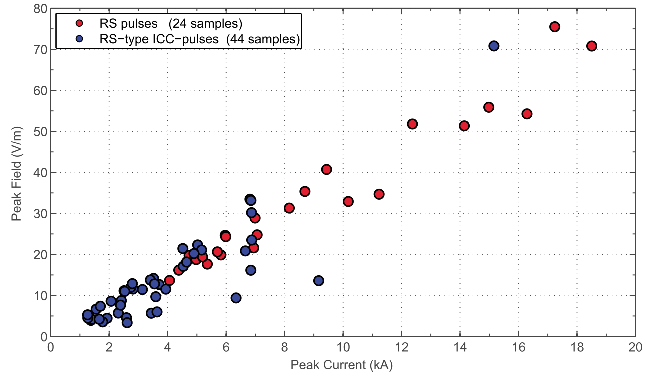

Figure 7. Scatter plot of electric field peak versus current peak for RS-type ICC-pulses (blue circles) and return strokes (red circles).

and electric fields associated with flashes to the Säntis tower. Their analysis showed that considering the real irregular terrain between the Säntis tower and the field measurement station, both the waveshape and amplitude of the simulated electric fields associated with return strokes were in excellent agreement with the measured waveforms. On the other hand, the assumption of a flat ground resulted in an underestimation of the peak electric field. Moreover, the electric field measured on the roof of a building might be affected by an enhancement that depends on several factors related to the building and on the position of the field sensor. The results of the analysis presented in *Li et al.* [2016] suggest an overall enhancement of the peak electric field of about a factor of 2. The results of *Li et al.* [2016] were found to be consistent with the recent study on the performance analysis of the European lightning detection network European Cooperation for Lightning Detection (EUCLID) [*Azadifar et al.*, 2016], in which it was shown that the peak current estimates provided by the EUCLID network were about 1.8 times higher than those from direct measurements.

Figure 8 presents the cumulative probability distribution of the current peak. The straight lines correspond to the lognormal approximations. Statistical characteristics for the current peak and field peak are summarized in Tables 1 and 2, respectively. We have also included in these tables the 90% confidence interval for the mean values. Note that in Table 2, the E-field peak values have been normalized to 100 km.

Figure 9 presents the scatterplot of the 10–90% E-field risetimes versus the 10–90% current risetimes excluding pulses with E-field peaks lower than about 10 V/m, for which the determination of the risetime might be significantly affected by noise (19 out of 44 RS-type ICC pulses were left out). For the plotted pulses (25 RS-type ICC-pulses and 24 return strokes), the radius of each circle is proportional to the current peak value.

The linear correlation coefficient between the E-field risetime and the current risetime for RS-type ICC-pulses is 0.99. Note that a very similar correlation coefficient (0.97) can be observed between the E-field risetime and current risetime for return stroke pulses.

It is worth noting that the current waveforms associated with both RS pulses and RS-type ICC pulses sometimes exhibit an initial peak followed by a larger, overall peak. A typical example of double-peak current and associated field waveforms is shown in Figure 10, in which the two peaks can be clearly seen. In the plots presented in Figure 9, the peak values and risetimes are associated with the initial peak of the current waveform.

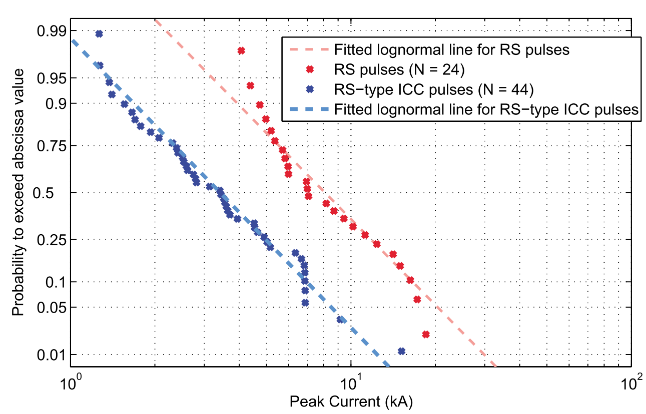

Figure 8. Cumulative peak current distributions for the return strokes (red) and RS-type ICC pulses (blue). The straight lines correspond to lognormal approximation.

5. Discussion on the Similarity Between RS-Type ICC Pulses and Return Stroke Pulses

The similarity of RS-type ICC pulses with return strokes suggests that these fast pulses are associated with the so-called mixed mode of charge transfer to ground, as defined in *Zhou et al.* [2015].

Zhou et al. [2015] suggested that ICC pulses are initiated by a downward

Table 1. Characterization of Current Peak (kA) for 44 RS-Type ICC Pulses and 24 Return Strokes

						Percentage Exceeding Tabulated Value		
	N	Min	Max	Mean	90% CI[a]	95%	50%	5%
ICC pulses	44	1.3	15.2	3.3	2.9–3.9	1.3	3.4	8.6
Return strokes	24	4.1	18.5	8.0	6.8–9.4	3.7	8.0	17.3
All	68	1.3	18.5	4.6	4.0–5.2	1.5	4.6	13.9

[a]90% CI is the 90% confidence interval of the mean value.

leader propagating along a previously created but decayed channel branch that connects to the grounded ICC-carrying channel. When the height of the junction point is in excess of a kilometer or so (in the cloud), an *M*-component mode of charge transfer occurs resulting in a long-front incident *M* wave. On the other hand, when the height of the junction point is relatively low (about 100 m or so from the tower top), a "mixed-mode" of charge transfer occurs, resulting in a leader/return stroke type process separated from the tower top by a relatively short conducting channel section (see Figure 15 of *Zhou et al*. [2015]). In the mixed mode, the return-stroke-like process can start at the tower top or at the junction point between the downward leader and the ICC carrying channel. In the latter case, the strike object can be viewed as being composed of the tower and the conducting channel section below the junction point, attached to the tower top. In either case, the upward propagating RS-like wave should be dominant.

In our data set presented in the previous section, the number of ICC-pulses (44) is larger than the number of return-strokes pulses (24). A similar trend was reported for the Peissenberg and Gaisberg Towers [*Fuchs et al*., 1998; *Diendorfer*, 2010], with 90 ICC-pulses versus 35 return strokes and 139 ICC-pulses versus 97 return strokes, respectively. Figure 11 shows an example of a current waveform recorded at the Säntis Tower with more than 20 ICC pulses and only one return stroke.

A question arises as to why the number of ICC pulses is significantly larger than the number of return strokes. An explanation for this can be given by making reference to the *M*-component and mixed modes of charge transfer to ground as defined in *Zhou et al*. [2015], in both of which a channel parallel to the existing one is involved in the charge transfer, with a common channel section between the junction point and the strike object (see Figure 15 of *Zhou et al*. [2015]). The difference between the two modes of charge transfer is essentially the height of the junction point, which is at a relatively short distance from the tower top (about 100 m or so) for the mixed-mode and at larger distances (in excess of a kilometer) for the *M*-component mode *Zhou et al*. [2015]. As evidenced by photographic observations [e.g., *Mazur and Ruhnke*, 2011], upward discharges can have multiple parallel channels involved in the charge transfer, which potentially results in a higher number of ICC pulses (whether due to *M*-component mode or mixed mode of charge transfer) relative to the number of "classical" leader/return sequences mostly following the main channel.

6. Summary and Conclusions

We examined fast superimposed on the initial continuous current of upward negative discharges. The study was based on experimental data consisting of lightning current waveforms recorded at the instrumented Säntis Tower in Switzerland, simultaneously with electric fields recorded at a distance of 14.7 km from the tower.

Table 2. Characterization of E-Field Peak (V/m) for 44 RS-Type ICC Pulses and 24 Return Strokes[a]

						Percentage Exceeding Tabulated Value		
	N	Min	Max	Mean	90% CI[b]	5%	50%	95%
ICC pulses	44	0.5	10.4	1.6	1.3–1.9	0.4	1.5	5.0
Return strokes	24	2.0	11.1	4.4	3.7–5.2	2.0	4.4	9.7
All	68	0.5	11.1	2.3	1.9–2.7	0.6	2.3	8.4

[a]Peak values are normalized to 100 km.
[b]90% CI is the 90% confidence interval of the mean value.

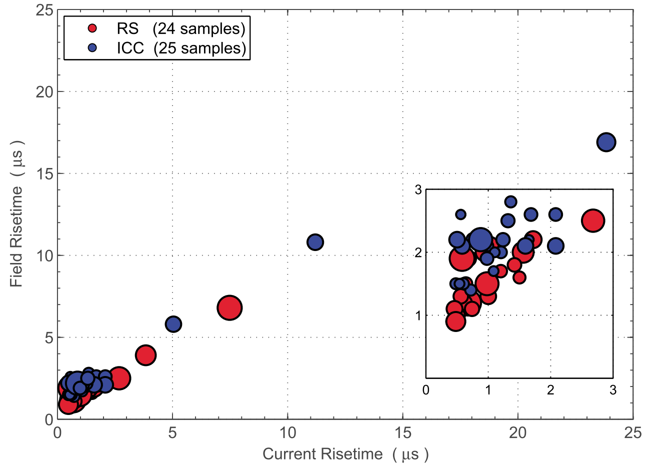

Figure 9. Scatterplot of electric field 10–90% risetime versus current 10–90% risetime for RS-type ICC pulses (blue) and return strokes (red). The radius of each circle is proportional to the associated peak current. The inset shows an expanded view of the scatterplot for risetimes less than 3 µs.

During the period of study (23 July to 28 October 2014), a total of 21 upward negative flashes were simultaneously recorded at the Säntis Tower and at the electric field measuring station.

Two different types of pulses superimposed on the initial continuous current were identified: (1) *M*-component-type pulses for which the microsecond-scale electric field pulse occurs significantly earlier than the onset of the current pulse and (2) fast pulses for which the onset of the field matches that of the current pulse. We presented an analysis of the currents and fields associated with these fast pulses (RS-type ICC pulses) and compared their characteristics with those of return strokes in the same flashes. The recorded flashes contained 44 RS-type ICC pulses and 24 return strokes.

The median current peaks associated with RS-type ICC pulses and return strokes were found to be 3.4 kA and 8 kA, respectively. The corresponding median E-field peaks normalized to 100 km were 1.5 V/m and 4.4 V/m.

The electric field peaks versus current peaks for the two types of events (RS-type ICC pulses and return strokes) were characterized by very similar linear regression slopes, namely, 3.67 V/(m kA) for the ICC pulses and 3.77 V/(m kA) for return strokes. Assuming the field-current relation based on the transmission line (TL) model, we estimated the apparent speed for both ICC pulses and return strokes to be about 1.4×10^8 m/s.

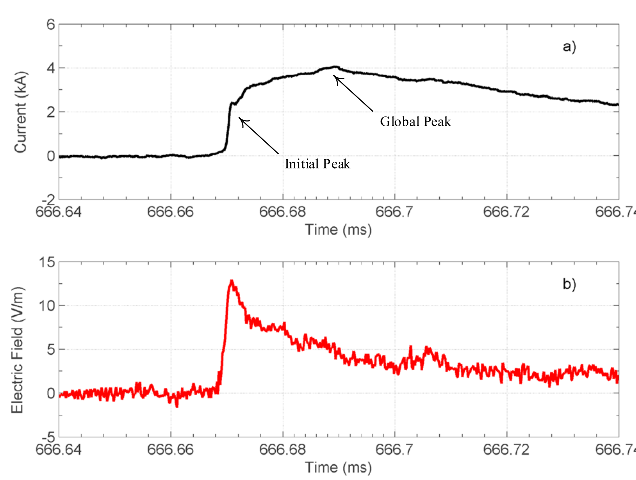

Figure 10. Double-peak current and associated E-field waveforms of RS-type ICC pulse for the flash that occurred on 21 October 2014 at 8:41 PM. (a) Current. (b) E-field.

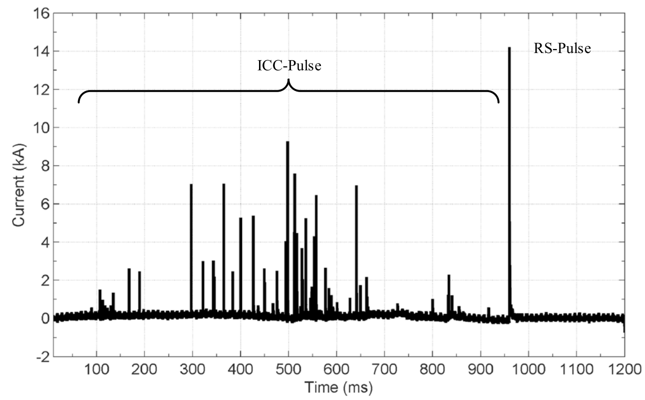

Figure 11. Current waveform associated with a flash that occurred on 21 October at 8:42 PM and exhibited many ICC pulses and only one return stroke.

Furthermore, a strong linear correlation is observed for RS-type ICC-pulses between the E-field risetime and the current risetime, similar to the relation observed between the E-field risetime and current risetime for return strokes.

The similarity of the RS-type ICC pulses with return strokes suggests that these pulses are associated with the mixed mode of charge transfer to ground.

Acknowledgments
The measured data on lightning currents and fields presented in this paper are accessible at the EMC Laboratory of EPFL (farhad.rachidi@epfl.ch). Financial support from the Swiss National Science Foundation (Project 200021_147058) is acknowledged. V.A. Rakov was supported in part by GRF Grant 14825.31.0023. Special thanks are due to Swisscom Broadcast (Walter Haas, Tony Heim, Johannes Inauen, Andreas Ryffel) and to Huber+Suhner (Cenk Koparan, Holger Karstensen) for their precious cooperation.

References

Azadifar, M., M. Paolone, D. Pavanello, F. Rachidi, C. Romero, and M. Rubinstein (2014), An update on the instrumentation of the Säntis Tower in Switzerland for lightning current measurements and obtained results, in *CIGRE International Colloquium on Lightning and Power Systems*, Lyon, France.

Azadifar, M., F. Rachidi, M. Rubinstein, M. Paolone, V. A. Rakov, D. Pavanello, S. Metz, and C. Romero (2015), Characteristics of electric fields of upward negative stepped leaders Int. Symp. Light. Protect., pp. 32–36, XIII SIPDA, Brazil.

Azadifar, M., F. Rachidi, M. Rubinstein,M. Paolone, G. Diendorfer, H. Pichler, W. Schulz, D. Pavanello, and C. Romero (2016), Evaluation of the performance characteristics of the European Lightning Detection Network EUCLID in the Alps region for upward negative flashes using direct measurements at the instrumented Säntis Tower, *J. Geophys. Res. Atmos.*, *121*, 595–606, doi:10.1002/2015JD024259.

Diendorfer, G. (2010), LLS performance validation using lightning to towers 21st Int. Light. Detect. Conf. (ILDC) & 3rd Int. Light. Meteorol. Conf. (ILMC), 19–20 April, Orlando, Florida.

Diendorfer, G., H. Pichler, and M. Mair (2009), Some parameters of negative upward-initiated lightning to the Gaisberg Tower (2000–2007), *IEEE Trans. Electromagn. Compat.*, *51*, 443–452.

Flache, D., V. A. Rakov, F. Heidler, W. Zischank, and R. Thottappillil (2008), Initial stage pulses in upward lightning: Leader/return stroke versus *M*-component mode of charge transfer to ground, *Geophys Res Lett.*, *35*, L13812, doi:10.1029/2008GL034148.

Fuchs, F., E. U. Landers, R. Schmid, and J. Wiesinger (1998), Lightning current and magnetic field parameters caused by lightning strikes to tall structures relating to interference of electronic systems, *IEEE Trans. Electromagn. Compat.*, *40*, 444–451.

Heidler, F. H., M. Manhardt, and K. Stimper (2013), The slow-varying electric field of negative upward lightning initiated by the Peissenberg Tower, Germany, *IEEE Trans. Electromagn. Compat.*, *55*(2), 353–361.

Li, D., M. Azadifar, F. Rachidi, M. Rubinstein, M. Paolone, D. Pavanello, S. Metz, Q. Zhang, and Z. Wang (2016), On lightning electromagnetic field propagation along an irregular terrain, *IEEE Trans. Electromagn. Compat.*, *58*(1), 161–171.

Mallick, S., et al. (2014), Performance characteristics of the NLDN for return strokes and pulses superimposed on steady currents, based on rocket-triggered lightning data acquired in Florida in 2004–2012, *J. Geophys. Res. Atmos.*, *119*, 3825–3856, doi:10.1002/2013JD021401.

Mazur, V., and L. H. Ruhnke (2011), Physical processes during development of upward leaders from tall structures, *J. Electrostat.*, *69*, 97–110.

Miki, M., V. A. Rakov, T. Shindo, G. Diendorfer, M. Mair, F. Heidler, W. Zischank, M. A. Uman, R. Thottappillil, and D. Wang (2005), Initial stage in lightning initiated from tall objects and in rocket-triggered lightning, *J. Geophys. Res.*, *110*, D02109, doi:10.1029/2003JD004474.

Miki, M., T. Miki, and T. Shindo (2012), Liminosity characteristics of initial continuous current pulses in upward lightning flashes 31th Int. Conf. Light. Protect., 2–7 Sep, Vienna.

Pichler, H., G. Diendorfer, and M. Mair (2010), Some parameters of correlated current and radiated field pulses from lightning to the Gaisberg Tower, *IEEJ Trans. Electr. Electron. Eng.*, *5*, 8–13, doi:10.1002/tee.20486.

Qie, X., R. Jiang, C. Wang, J. Yang, J. Wang, and D. Liu (2011), Simultaneously measured current luminosity and electric field pulses in a rocket-triggered lightning flash, *J. Geophys. Res.*, *116*, D10102, doi:10.1029/2010JD015331.

Rachidi, F., and R. Thottappillil (1993), Determination of lightning currents from far electromagnetic fields, *J. Geophys. Res.*, *98*, 18,315–18,320, doi:10.1029/93JD01616.

Rakov, V. A. (2007), Lightning return stroke speed, *J. Lightning Res.*, *1*, 80–89.

Rakov, V. A., and M. A. Uman (2003), *Lightning: Physics and Effects*, Cambridge Univ. Press, New York.

Rakov, V. A., D. E. Crawford, K. J. Rambo, G. H. Schnetzer, M. A. Uman, and R. Thottappillil (2001), M-component mode of charge transfer to ground in lightning discharges, *J. Geophys. Res.*, *106*, 22,817–22,831.

Romero, C., M. Paolone, M. Rubinstein, F. Rachidi, A. Rubinstein, G. Diendorfer, W. Schulz, B. Daout, A. Kälin, and P. Zweiacker (2012), A system for the measurements of lightning currents at the Säntis Tower, *Electr. Power Syst. Res.*, *82*, 34–43.

Romero, C., F. Rachidi, M. Paolone, and M. Rubinstein (2013), Statistical distributions of lightning currents associated with upward negative flashes based on the data collected at the säntis tower in 2010 and 2011, *IEEE Trans. Power Delivery*, *28*(3), 1804–1812.

Tran, M. D., V. A. Rakov, T. Ngin, W. R. Gamerota, J. T. Pilkey, M. A. Uman, and D. M. Jordan (2013), Microsecond-scale electric field pulses associated with lightning *M*-components, Abstract AE13B-0356, AGU, Fall Meet. 2013.

Winn, W. P., E. M. Eastvedt, J. J. Trueblood, K. B. Edens, G. D. Aulich, S. J. Hunyady, and W. C. Murray (2012), Luminous pulses during triggered lightning, *J. Geophys. Res.*, *117*, D10204, doi:10.1029/2011JD017105.

Zhou, H., V. A. Rakov, G. Diendorfer, R. Thottappillil, H. Pichler, and M. Mair (2015), A study of different modes of charge transfer to ground in upward lightning, *J. Atmos. Sol. Terr. Phys.*, *125–126*, 38–49.